Singlet-triplet anticrossings in 4He. III. Separation and mixing of the n=3-8 1D and 3D states

J. Derouard, R. Jost, M. Lombardi, T. A. Miller, R. S. Freund

Singlet-triplet anticrossings in ^{4}He. III. Separation and mixing of the $n = 3$–8 ^1D and ^3D states

J.Derouard,* R. Jost,* and M. Lombardi*
Laboratoire de Spectrometrie Physique,† Universite Scientifique at Medicale de Grenoble, B.P. 53-38041 Grenoble Cedex, France

T. A. Miller‡ and R. S. Freund‡
Bell Laboratories, Murray Hill, New Jersey 07974
(Received 2 February 1976)

The method of singlet-triplet anticrossing has been extended to the $n\,^{1\text{-}3}D$ levels of ^{4}He with $n = 3$, 4, and 5. We measure both the zero-field singlet-triplet separation with a higher accuracy than optical measurements, and the antisymmetric part of the spin-orbit coupling between singlet and triplet states. The agreement with many-body perturbation calculations for singlet-triplet intervals and with the hydrogenic approximation for spin-orbit coupling is fairly good even for low-n states. Values of singlet-triplet mixing in the $n = 3$–8 D states, derived directly from the experimental results, are significantly more accurate than previous experimental and theoretical values.

I. INTRODUCTION

The observation of level anticrossings is a simple and relatively precise method of studying atomic and molecular excited states. It has recently been applied by our two groups [hereafter referred to as BTL (Bell Labs) and Grenoble] to the study of nd Rydberg states of ^{4}He,[1,2] H_2,[3,4] and $^4He_2$.[5]

This article is the third in a series on the $n\,^{1\text{-}3}D$ levels of ^{4}He. The first two[1,2] will henceforth be referred to as I and II. Here we present results on the $n = 3$–6 $^{1\text{-}3}D$ levels of ^{4}He, for which we measure both the singlet-triplet separation and the spin-orbit coupling. The experiments are carried out under different conditions by our two groups. The results agree and so provide reliable tests of the theory recently presented by Chang and Poe[6-9] as regards the $n\,^1D$-$n\,^3D$ separation, of previous estimates of singlet-triplet mixing for such states, and of the hydrogenic approximation as regards the spin-orbit coupling. Results for $n = 6$–8 from I and II are included in the tables.

II. EXPERIMENTAL

Observation of $n\,^{1\text{-}3}D$ anticrossings for $n \leq 5$ requires magnetic fields of several tesla (1 T = 10 kG), which cannot be attained by classical electromagnets; thus the experiments were carried out in Bitter coils at MIT by the BTL group and at the Service National des Champs Intenses by the Grenoble group.

At Grenoble, the apparatus is similar to that already used for H_2.[3] Helium contained in a sealed Pyrex cell is excited by a capacitive discharge (Lecher line) at 150 MHz (Fig. 1).[10] In a high magnetic field, the discharge can be started only at a pressure greater than 5×10^{-2} Torr; hence the measurements were taken in the 5×10^{-2}–3-Torr range. A fairly important oscillating electric field exists within this discharge; its effective value has been measured as 20–100 V/cm according to the pressure and the discharge current. The emitted light, which is observed parallel to the magnetic field, is successively analyzed by a rotating birefringent plate (frequency $\simeq$ 100 Hz) and a fixed linear polarizer, and then is wavelength selected by a monochromator and detected by a thermoelectrically cooled and magnetically shielded EMI 9558 photomultiplier. One obtains simultaneously the polarization (modulated signal) detected by a lock-in amplifier (PAR 124) and the total light intensity for the singlet or triplet (according to the wavelength selected). These two signals are recorded on two multichannel analyzers (200 channels each) for numerical treatment. In general, each pair of curves is obtained by accumulating four sweeps

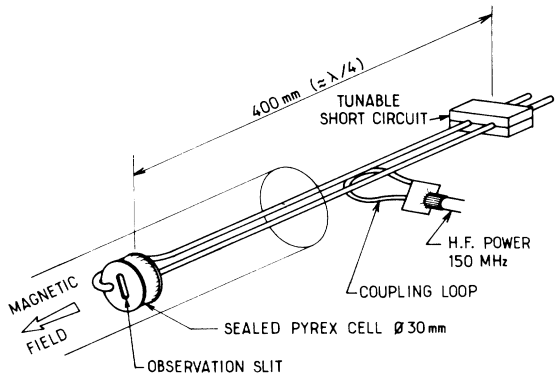

FIG. 1. Lecher line used by Grenoble to produce a hf discharge in the helium cell.

each lasting 200 sec.

The magnetic field is measured by a Hall-effect probe with a precision of 1 part in 10^3. The inhomogeneity of the field is of the order of 1 part in 10^3 over the volume of the cell. The temporal fluctuations in the power supply were better than 1 part in 10^4 over several minutes.

At MIT, a Bitter coil was chosen for high spatial homogenity, roughly 1 part in 10^4 over the 1-cm^3 sample volume at fields up to 13 T. As temporal fluctuation in the power generators were about 1 part in 10^3, however, it was necessary to use a stabilization circuit. In this circuit, a 700-turn coil inside the Bitter coil produces a voltage proportional to a magnetic flux change (dB/dt). This voltage controls a ±20-A power supply which drives a pair of coils built into the Bitter coil but independent of it. The resulting field is stable to 1 part in 10^5 over a period of several seconds and 1 part in 10^4 over several minutes. This stabilizing circuit is necessary for the NMR measurements described below.

Magnetic field measurements were made by a Hall probe which was frequently calibrated at the magnetic field of interest by NMR. The NMR system was similar to one designed by Adams.[11] It works on the balanced hybrid or "magic T" principle. A probe with $CuCl_2$-doped water constitutes one arm of the T. Power absorption at the proton resonance frequency unbalances the bridge, and the resulting signal is amplified, detected, and displayed on a scope which is swept synchronously with the 1-KHz FM of the radiofrequency source. NMR signals have been detected over the range of 1–12 T with a single sample probe.

The vacuum chamber was a 2-m-long, 5-cm-diam stainless-steel vacuum tube, pumped from one end to a base pressure of ~10^{-4} Torr. Inside the Bitter coil (Fig. 2), electrons are emitted by a 1-cm^2 indirectly heated $BaSrCO_3$ cathode, are accelerated by a grid to 100 eV, and travel along the magnetic field to a (grounded) collector. Light from the interaction region is reflected by a 45° mirror into a 1-cm-diam, 70-cm-long solid fused silica light pipe. Light from the light pipe is focused on the entrance slit of a Spex $\frac{3}{4}$-m monochromator and finally detected by a thermoelectrically cooled and magnetically shielded EMI 9658 photomultiplier.

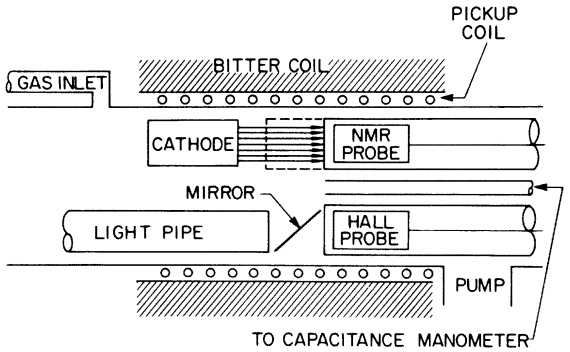

FIG. 2. Apparatus used by the BTL group at the MIT Bitter Magnet Laboratory. The tube which holds the NMR probe is moved into the interaction region (dashed lines) for magnetic field calibration. It also serves as the electron collector. A control grid ~0.5 mm from the cathode is not shown.

Final measurements of anticrossing positions and widths were made by using the triangular ramp output of a signal averager to sweep the unstabilized magnetic field synchronously with the channel number. The sweep width and Hall probe were calibrated with the NMR probe before measurements on each state and the absolute field was measured at several channels of the signal averager with the calibrated Hall probe before and after each measurement. The calibrations were checked roughly every hour with the NMR probe, since the Hall probe drifted by up to several tens of gauss. No corrections are required for magnetic field gradients, because Hall probe calibrations were made by moving the NMR probe directly into the interaction region.

Because the position and width of anticrossing lines can be affected by collisions and electric fields, it would have been desirable to make measurements at several pressures and electron currents and extrapolate to zero. Limited magnet time prevented this procedure, however. Measurements were therefore made at 5 mTorr pressure and ~0.5 mA current, values which previous work has shown to give data at the zero-pressure and -current limits. As a check, remeasurement of the $n = 6\,^{1,3}D$ anticrossing gave results essentially in agreement with II.

III. THEORY

A. Introduction

The theory has been expounded in detail in I. Let us recall here the main lines of thought.

In an $L = 2$ subspace the Hamiltonian of the He atom can be written

$$\mathcal{H} = \mathcal{H}_{\text{el st}} + \mathcal{H}_z + \mathcal{H}_1 + \mathcal{V}, \tag{1}$$

where $\mathcal{H}_{\text{el st}}$ is the electrostatic part and $\mathcal{H}_z$ the linear Zeeman Hamiltonian. These two terms lead to the $(L, M_L; S, M_S)$ energy levels in a decoupled representation. (See the energy-level diagrams in Fig. 1 of I and Fig. 1 of II.) $\mathcal{H}_1$ consists of small terms (fine structure, quadratic

TABLE I. Values (in MHz) of the diagonal spin-orbit A and spin-spin b parameters in the nd^3D states, and the off-diagonal spin-orbit parameter $\mathfrak{A}$ between the nd^1D and nd^3D states.

Level	$\mathfrak{z}_0$ [a]	$\mathfrak{z}_1$ [a]	$\mathfrak{z}_2$ [a]	A_{theor} [b]	A_{expt}	b_{theor} [b]	b_{expt}	$\mathfrak{A}_{\text{theor}}$ [b]	$\mathfrak{A}_{\text{expt}}$ [c]
$3d$	866	430	14	−204	−216.4 ± 0.1 [d]	491	509.6 ± 0.2 [d]	645	639 ± 30
$4d$	365	181	8	−84.2	−91.7 ± 0.1 [d]	207	212.4 ± 0.2 [d]	271	267 ± 20
$5d$	187	93	5	−43.7	−47.0 ± 0.3 [e]	107	107.3 ± 0.8 [e]	139	137 ± 10
$6d$	108	54	3	−25.2	−27.8 ± 0.5 [e]	61.7	63.1 ± 0.8 [e]	80	80.1 ± 6
$7d$	68	34	···	−17.0	−15.5 ± 2.3 [f]	38.9	34.7 ± 6.0 [f]	51	50.5 ± 4
$8d$	46	23	···	−11.5	···	26.3	···	35	36.0 ± 4

[a] Reference 12.
[b] Derived from Eq. (4), (5), or (6).
[c] This work.
[d] Derived from fine-structure measurements of Ref. 13.
[e] Derived from $\Delta\nu_{12}$ of Ref. 14 and $\Delta\nu_{23}$ of Ref. 15.
[f] Derived from $\Delta\nu_{12}$ of Ref. 16 and $\Delta\nu_{23}$ of Ref. 15.

Zeeman, and Stark effects) which commute with the total electronic spin $\vec{S}=\vec{s}_1+\vec{s}_2$ ($\vec{s}_i$ is the spin of the ith electron) and roughly speaking does no more than slightly shift the levels (these terms are imprecisely but conveniently called second-order effects).

The last term $\mathcal{V}$ is the part of the spin-orbit interaction which couples singlets and triplets, $\mathcal{V}=\mathfrak{A}\vec{L}\cdot\vec{S}$. L is the total orbital angular momentum, $\vec{S}=\vec{s}_1-\vec{s}_2$, and $\mathfrak{A}$ is defined by Eq. (7) of I. The ^1D and ^3D states are only weakly mixed in zero magnetic field, since $\mathfrak{A}$ is much smaller than their separation. At certain nonzero fields, however, some sublevels approach each other and become mixed through the interaction $\mathcal{V}$. However, they do not actually cross. Rather, they repel each other; the resulting phenomenon is called anticrossing. The resulting population changes can be observed as changes in the intensity of light emitted by the ^1D and ^3D levels.

B. Second-order effects

Four anticrossings are allowed ($\Delta M_J=0$) between singlet states with $M_L=2,1,0,-1$, $M_S=0$, and triplet states with $M_L=1,0,-1,-2$, $M_S=1$, and would occur for exactly the same value of the field were it not for the small displacements induced by $\mathcal{H}_1$. These second-order effects can conveniently be divided into three sources: fine-structure effects (spin-orbit and spin-spin coupling), quadratic Zeeman effects resulting from the anisotropy of the atom's diamagnetic susceptibility, and Stark effects. The formulas for these displacements were given in I and II.

The fine-structure Hamiltonian (spin orbit and spin spin) is expressed as a function of the constants A and b. These are experimentally determined from the zero-field fine-structure-intervals measurements (Table I). The relationships are

$$\Delta\nu_{13}=\tfrac{5}{8}b-5A\,, \tag{2}$$

$$\Delta\nu_{23}=-(3A+\tfrac{9}{8}b)\,. \tag{3}$$

In the hydrogenic approximation, one supposes that the wave functions are linear combinations of Slater determinants built on the single configuration ($1s$, nd), where $1s$ and nd are hydrogen-like functions with, respectively, $Z=2$ and $Z=1$ for the nuclear charge. As this approximation is of considerable utility it is convenient at this point to express the spin-orbit and spin-spin parameters A, b, and $\mathfrak{A}$ in terms of radial integrals[12] $\mathfrak{z}_0$, $\mathfrak{z}_1$, and $\mathfrak{z}_2$,

$$A=\tfrac{1}{2}\mathfrak{z}_0-\tfrac{3}{2}\mathfrak{z}_1+\tfrac{3}{5}\mathfrak{z}_2\,, \tag{4}$$

$$b=\tfrac{8}{7}\mathfrak{z}_1\,, \tag{5}$$

$$\mathfrak{A}=\tfrac{1}{2}\mathfrak{z}_0+\tfrac{1}{2}\mathfrak{z}_1-\tfrac{1}{5}\mathfrak{z}_2 =A+\tfrac{7}{4}b-\tfrac{4}{5}\mathfrak{z}_2\,, \tag{6}$$

where

$$\mathfrak{z}_0(nd)=\tfrac{1}{2}\alpha^2\langle nd|r^{-3}|nd\rangle\,,$$

$$\mathfrak{z}_1(nd)=\tfrac{1}{2}\alpha^2\langle nd(r_1)1s(r_2)|r_1^{-3}\epsilon(r_1-r_2)|nd(r_1)1s(r_2)\rangle\,,$$

$$\mathfrak{z}_2(nd)=-\tfrac{1}{2}\alpha^2\langle nd(r_1)nd(r_2)|\frac{r_<}{r_>^4}\,r_2\frac{\partial}{\partial r_1}|1s(r_1)1s(r_2)\rangle\,,$$

$$\epsilon(x)=\begin{cases}1, & \text{if } x>0\,,\\ 0, & \text{if } x<0\,;\end{cases}$$

$r_<=\min(r_1,r_2)$, $r_>=\max(r_1,r_2)$, and α is the fine-structure constant $e^2/\hbar c$.

Comparison between theory and experiment[13-16] (Table I) shows that the hydrogenic approximation is fairly good, even for the lowest levels. This justifies use of the hydrogenic approximation to calculate the other second-order effects, for which measurements are unavailable.

As regards the Stark effect, we consider the

transverse $\mathcal{F}_\perp$ and longitudinal $\mathcal{F}_\parallel$ parts of the electric field. $\mathcal{F}_\perp$ is due to the motional field seen by atoms moving in the magnetic field H_0 with thermal velocity v. We assume that atoms are in thermal equilibrium at 300 °K, so that the transverse effective field is $\mathcal{F}_\perp \simeq H_0(2kT/M)^{1/2}$.

In the BTL experiments $\mathcal{F}_\parallel$ is negligible, but this is not the case for the Grenoble experiments, where hf discharge excitation was used. Taking into account only the perturbation of the neighboring F states, the shift of the n, L, M, S, M_S state is[17] (with the notation of I).

$$E_2^{\text{Stark}} = \left(\frac{3nea_0}{4}\right)^2 \frac{[n^2-(L+1)^2]}{(2L+1)(2L+3)} \left[\left(\frac{(L+M+1)(L+M+2)}{{}^{1,3}E_{n,L,M} - {}^{1,3}E_{n,L+1,M+1}} + \frac{(L-M+1)(L-M+2)}{{}^{1,3}E_{n,L,M} - {}^{1,3}E_{n,L+1,M-1}} \right) \mathcal{F}_\perp^2 + \frac{4(L+M+1)(L+1-M)}{{}^{1,3}E_{n,L,M} - {}^{1,3}E_{n,L+1,M}} \mathcal{F}_\parallel^2 \right]. \quad (7)$$

The quadratic Zeeman effect can be treated exactly as before. The results of the calculations of all of the second-order anticrossing shifts are given in Tables II and III. For the Stark effect calculations, the energies of the nF levels are taken from Martin.[18]

C. Shapes and widths of anticrossing signals

The shape of an anticrossing signal, as given in I, is

$$I_{MM'} = \frac{-2\,|V_{SM,TM'}|^2(\rho^0_{SM}\tau_S - \rho^0_{TM'}\tau_T)(K_{SM}\tau_S - K_{TM'}\tau_T)}{4\,|V_{SM,TM'}|^2 f_\tau^2 + \hbar^2\bar{\Gamma}^2 + g_e^2\mu_0^2(H-H_0)^2}, \quad (8)$$

where

$$V_{SM,TM'} = \langle L=2, M_L, S=0, M_S=0 \,|\, \mathcal{V} \,|\, 2, M_L-1, 1, 1\rangle$$

is the matrix element of the spin-orbit coupling (expressed in the decoupled representation), $\rho^0_{S(T),M}$ is the diagonal element of the density matrix for the Mth level of the singlet (triplet) state, $K_{S(T),M}$ is the intensity of emission from the Mth level of the singlet (triplet) state as detected by the experimental apparatus, $\tau_{S(T)}$ is the radiative lifetime of the singlet (triplet) state,

$$\bar{\Gamma} = 1/\bar{\tau}, \quad f_\tau = (\tau_S\tau_T/\bar{\tau}^2)^{1/2} = (\bar{\Gamma}^2/\Gamma_S\Gamma_T)^{1/2},$$

$$\bar{\tau}^{-1} = \tfrac{1}{2}(\tau_S^{-1} + \tau_T^{-1}) = \bar{\Gamma} = \tfrac{1}{2}(\Gamma_S + \Gamma_T),$$

$g_e = g_L - g_S = -1.002\,46$ is the effective Lande factor, $g_L = 1 - m/M = 0.999\,86$, and $g_S = 2.002\,32$.

The width [full width at half-maximum (FWHM)] of an anticrossing undergone by a pair of sublevels $|M_L$, singlet$\rangle$ and $|M_L - 1$, triplet$\rangle$ is

$$\Delta\nu_c = 2(4\mathcal{C}^2 f_M^2 f_\tau^2 + \hbar^2\bar{\Gamma}^2)^{1/2}, \quad (9a)$$

where, for ^1D-^3D anticrossings,

$$f_M = \begin{cases} \sqrt{2}, & \text{for } M_L = 2 \text{ or } -1, \\ \sqrt{3}, & \text{for } M_L = 1 \text{ or } 0. \end{cases} \quad (9b)$$

In the present case the values of $\mathcal{C}$ (Table I), τ, and f_τ (Table IV) are such that

$$4\mathcal{C}^2 f_M^2 f_\tau^2 \gg \hbar^2\bar{\Gamma}^2,$$

so the anticrossing widths are given quite accurately by

TABLE II. Numerical values for the difference (singlet minus triplet, in MHz) in the levels $M_L, M_S = 0$ of the singlet and $M_L - 1$, $M_S = 1$ of the triplet states at the anticrossing field due to second-order effects. The singlet $M_L = 2$ anticrossing falls at highest field.

Singlet	M_L	Quadratic Zeeman	Fine structure	Motional Stark	Total
$3d$	2	28.4	280.1	0	308.5
	1	9.5	127.4	0	136.8
	0	−9.5	−152.7	0	−162.2
	−1	−28.4	−560.1	0	−588.5
$4d$	2	38.0	118.2	−0.3	155.8
	1	12.7	53.1	−0.2	65.6
	0	−12.7	−65.1	−0.2	−77.9
	−1	−38.0	−236.4	−0.2	−274.6
$5d$	2	33.8	60.4	−0.7	93.5
	1	11.3	26.8	−0.5	37.6
	0	−11.3	−33.5	−0.5	−45.3
	−1	−33.8	−120.8	−0.6	−155.2
$6d$	2	27.5	35.6	−1.1	62.0
	1	9.2	15.7	−0.9	24.0
	0	−9.2	−19.9	−0.9	−30.0
	−1	−27.5	−71.3	−1.2	−100.0

TABLE III. Numerical values for the difference (singlet minus triplet, in MHz) in the levels $M_L, M_S = 0$ of the singlet and $M_L - 1, M_S = 1$ of the triplet states at the anticrossing field due to longitudinal Stark effect for an effective value of $\mathcal{F}_\parallel$ of 60 V/cm.

Singlet M_L	$3d$	$4d$	$5d$	$6d$
2	···	0.23	1.25	4.8
1	···	−0.36	−2.9	−12.4
0	···	−0.81	−6.0	−25.1
−1	···	−1.13	−8.0	−33.5

TABLE IV. Radiative lifetimes and the function f_τ for the D states of He. The $3d$-$5d$ values are calculated from the table of Wiese *et al.* (Ref. 19). The $6d$-$8d$ values are calculated from Table I of Gabriel and Heddle (Ref. 20). The $3d$-$5d$ lifetimes calculated from Gabriel and Heddle agree with the Wiese values, within the stated error, so we assume that the $6d$-$8d$ values are of comparable accuracy.

Level	τ_{singlet}	τ_{triplet}	$f_\tau = (\tau_S\tau_T)^{1/2}\frac{1}{2}(1/\tau_S + 1/\tau_T)$
$3d$	15.67 ± 0.47	14.16 ± 0.42	$1.001^{+0.002}_{-0.001}$
$4d$	36.6 ± 1.2	31.5 ± 0.9	$1.003^{+0.003}_{-0.002}$
$5d$	71.6 ± 20	60.7 ± 1.6	$1.003^{+0.003}_{-0.002}$
$6d$	123.0	107.1	1.002
$7d$	207.5	145.4	1.016
$8d$	296.7	207.5	1.016

$$\Delta\nu_c \cong 4|\mathcal{A}|f_M f_\tau . \tag{10}$$

The relative intensities of the four anticrossings are determined by populations of the M levels and anisotropies in the radiation patterns. We have no measurements of the rates of alignment induced by electron bombardment in high magnetic field. Nevertheless, measurements of the Hanle effect carried out at pressures of a few 10^{-1} Torr using hf discharge excitation showed fairly weak alignment rates, less than 1%.[10] For BTL experiments (low pressure), alignment is possibly more important and may be of the order of 10%.[10] However, we assume that all of the Zeeman sublevels are similarly populated. As the second-order separations are rather small compared with the anticrossing widths, this approximation will not have large consequences. The relative intensities for observation parallel or perpendicular to the magnetic field[21] are given in Table V.

The anticrossing signal is then composed of four Lorentzian curves which are (slightly) separated by the intervals given in Table II. Their relative full widths at half-height are in the proportions $\sqrt{2}$ and $\sqrt{3}$, as given by Eq. (9b). Their relative intensities depend on the conditions of electron excitation and on the direction of observation (Table V).

It is worthwhile to explicitly state the conditions under which the calculated width and intensity factors may not be entirely accurate. As mentioned before, alignment in the excitation could invalidate the intensity relation. Secondly, pressure effects could alter the line widths and intensities, as discussed in Sec. IV B. However, since the pressure in the BTL experiments is quite low, neither the widths nor the intensities are likely to be radically altered. As the second-order corrections are also small, almost certainly no appreciable error in the final field positions are introduced by the above assumptions concerning intensity and width.

IV. RESULTS

A. BTL data

Results of the BTL measurements are given in Table VI. Each reported line position is the average of two or three independent runs. The error is estimated as 5% of the linewidth. This, we feel, is the best that the line center can be located, even though the standard deviations of the individual measurements are considerably smaller. A typical pair of anticrossings is shown in Fig. 3.

Line-shape simulations, based on the theory of Sec. III, are used to determine the values of $|\mathcal{A}|f_\tau$. The error limits are determined by simulations which clearly give lines wider or narrower than those observed. The small difference between the $|\mathcal{A}|f_\tau$ values measured at MIT and at BTL on $n = 6$ probably results from two causes: The MIT value may be slightly too large due to the pressure and current which were not extrapolated to zero and due to the temporal magnetic field instability; these effects should be less important for lower n. The BTL value[2] may be slightly too small as computer line-shape fits indicate that the previous manual determinations may have slightly (~2–3%) but systematically underestimated the true width. The average value is probably the best and is henceforth used. Linewidths are calculated from the values of $|\mathcal{A}|f_\tau$.

TABLE V. Relative intensities of emission from the ^{1-3}D anticrossing levels (Ref. 21, pp. 63 and 91) for observation parallel and perpendicular to the magnetic field.

Singlet			Triplet		
M_L	$I_\perp$	$I_\parallel$	M_L	$I_\perp$	$I_\parallel$
2	6	6	1	9	3
1	9	3	0	10	2
0	10	2	−1	9	3
−1	9	3	−2	6	6

TABLE VI. Results of $n\,^{1-3}D$ anticrossing measurements. H_{anti} is the anticrossing position in the hypothetical absence of second-order effects. The last column gives the singlet-triplet separation (in GHz) with respect to the center-of-gravity of the ^3D levels derived from the average field.

Level	Anticrossing position (G) Singlet	Triplet	$\|\mathcal{A}\|f_T$ (MHz)	Width (G) of observed line (FWHM) Singlet	Triplet	H_{anti} Singlet	Triplet	Separation
$3d$	72 806 ± 160	72 674 ± 160	640 ± 30	3021 ± 130	3010 ± 130	72 895	72 682	102.13 ± 0.2
$4d$	42 069 ± 70	42 068 ± 70	268 ± 20	1281 ± 85	1275 ± 85	42 109	42 068	59.05 ± 0.08
$5d$	24 272 ± 35	24 283 ± 35	137 ± 10	664 ± 42	661 ± 42	24 294	24 281	34.078 ± 0.045
$6d$	14 904 ± 21	14 907 ± 21	83 ± 5	406 ± 21	404 ± 21	14 919	14 905	20.923 ± 0.030
$6d$ [a]	14 899 ± 15		77.5 ± 4	390 ± 20		14 907 [b]		20.916 ± 0.021
$7d$ [a]	9 710 ± 20		50.5 ± 4	254 ± 20		9 714 [b]		13.629 ± 0.028
$8d$ [a]	6 650 ± 25		36.0 ± 4	180 ± 20		6 652 [b]		9.334 ± 0.035

[a] Reference 2. The position for $n = 8$ was incorrectly given in Ref. 1 and 2 as 6750.
[b] Second-order corrections extrapolated from fits to $n = 3$–6 Bitter magnet data.

The singlet and triplet widths differ because of the unequal intensities and line separations. Shifts of the simulated line due to second-order effects were also calculated from $|\mathcal{A}|f_T$ and were used to determine the line position in the hypothetical absence of second-order effects. Theory predicts that these singlet and triplet positions should be the same, which they are, within the stated experimental error.

The singlet-triplet separation in zero magnetic field is calculated from the average (H_{av}) of the singlet and triplet line positions in the absence of second-order effects (Table VI) by the formula

$$\Delta E = g_e \mu_0 H_{av} . \tag{11}$$

The resulting separations (Table VI) are, with respect to the center of gravity of the triplet fine-structure levels, similar to the values reported in I and II. In Sec. V A we give a ΔE which refers to the $^1D_2$-$^3D_2$ separation.

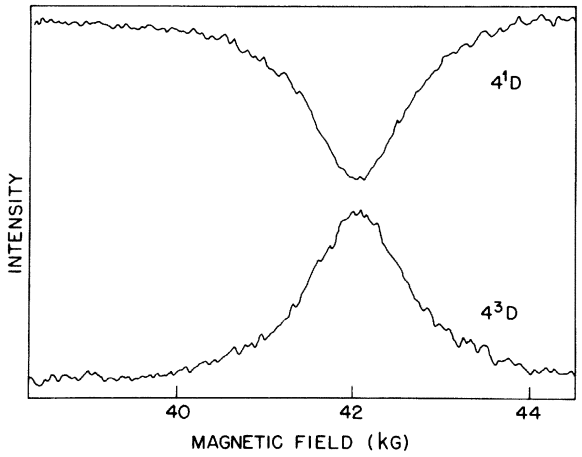

FIG. 3. Experimental anticrossing signals obtained by the BTL group at MIT.

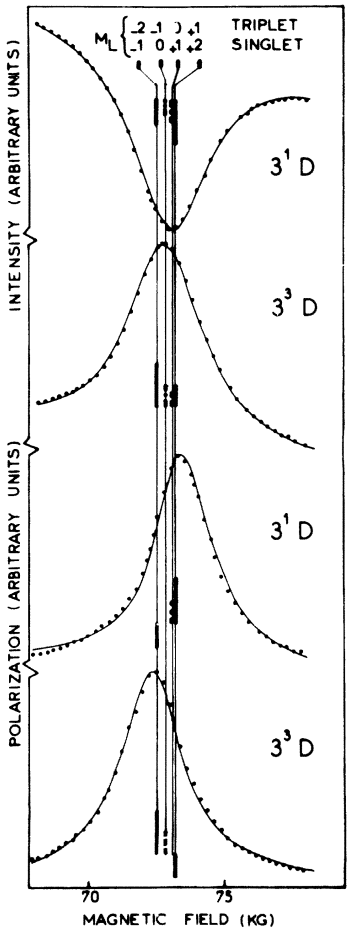

FIG. 4. Experimental anticrossing signals (dotted curves) and corresponding fitted curves (continuous line) obtained by the Grenoble group. For the sake of clarity only half of the dots are shown. The different components are shown in relative intensity and position by vertical lines, solid lines for components whose width is $\sqrt{2}\mathcal{A}f_T$ and dashed lines for components whose width is $\sqrt{3}\mathcal{A}f_T$. The pressure of the helium cell was about 10^{-1} Torr.

The values of $\mathcal{C}$ derived from $|\mathcal{C}|f_\tau$ and f_τ from Table IV are given in Table I, where the hydrogenic calculations of them are also given.

B. Grenoble data

Qualitatively there are four experimental curves (intensity, polarization, singlet, and triplet) to determine the relative positions of the four components of the anticrossing. In Fig. 4 we see that there is an experimental splitting of the various curves of the order of 30% of their width. This gives hope that one can recover the individual components by a global least-squares fit of all four curves.

However, we were disturbed by pressure effects and by longitudinal Stark effects. Concerning the pressure effects, consider the isotropic relaxation under the effect of transfers between Zeeman sublevels of different M_L in each $(n;L;S,M_S)$ subspace. It can be described by relaxation coefficients $\gamma^{(k)}$ of the kth-order multipoles.[22-24] This is justified here because the inverse of the collision time (of the order of a few 10^{11} to a few 10^{12} sec^{-1}) is large compared to the separation between Zeeman sublevels in high magnetic field[23,24] (which is of the order of a few 10^{10} to a few 10^{11} sec^{-1}, or a few times the singlet-triplet separation). Roughly speaking, $1/\gamma^{(0)}$ is of the order of the time the atom spends in the $(n;L;S,M_S)$ subspace (relaxation of the population), which is the radiative lifetime shortened by collision quenching; $1/\gamma^{(k)}$ with $k\neq 0$ is of the order of the time the atom spends in the M_L state inside the $(n;L;S,M_S)$ subspace. This latter time can of course be shorter than the former, and thus $\gamma^{(k)}>\gamma^{(0)}$, as the atom could be depolarized while it is in an excited state owing to collision with another atom in its ground state. We can write $\gamma^{(k)}=(1+P)\gamma$, where P is proportional to the pressure and to the depolarization cross section; γ is the radiative lifetime. Then we can show by calculation on a computer of the evolution of the atomic system reduced to the $(n;L=2;S=0,M_S=0)+(n;L=2;S=1,M_S=1)$ subspace that the anticrossing signal is roughly multiplied in width by a factor of the order of $[(\gamma^{(k)}+\gamma^{(0)})/2\gamma^{(0)}]^{1/2}$. We assumed all $\gamma^{(k)}$ with $k\neq 0$ to be equal, which is a fairly good approximation; for several atomic species, measurements or calculations have always given values which are equal to within 20%.[24-27] We assumed also that the relaxation coefficients are the same for the singlet and the triplet, which is probably also a good approximation, since singlet and triplet wave functions are very similar for Rydberg states. Using the depolarization cross sections already measured,[26,27] we find that the width of the anticrossing signal is doubled for a pressure of the order of 3 Torr for the $3\,^{1-3}D$ anticrossings, and 0.5 Torr for the $6\,^{1-3}D$ anticrossings. This applies to pressures which are not too high, at the limit at which the quenching is negligible, i.e., $\gamma^{(0)}$ is not too far from the radiative lifetime (typically from a few Torr to a few tens of Torr).

At the same time, the anticrossing signal corresponding to one particular sublevel is transferred equally to the four other Zeeman sublevels, which have different directional properties. This clearly falsifies the hypotheses invoked for the BTL data, concerning the relative intensity of the various components of the signal.

We have thus fitted only recordings made on cells at relatively low pressure, about 10^{-1} Torr. But the oscillating electric field of the discharge may be rather great for these pressures and thus may produce a noticeable Stark effect, at least for levels where $n\geq 6$ (Table III).

Finally, we fitted our observed signals by a curve calculated according to the preceding theory. The relative positions and intensities of the various components of the anticrossing were fixed, but we left as variables the parameters $\mathcal{C}$ (width), the absolute position H_0 of the anticrossing without second-order effects, and, for the $6\,^{1-3}D$ anticrossing, the electrical longitudinal field $\mathcal{F}_{\parallel}$, as its effective value during the experiment was unknown. Of course, other nonphysical parameters were fitted, such as baseline and scale for each of the four curves of an anticrossing $n\,^{1-3}D$.

V. DISCUSSION

A. Singlet-triplet separation

Experimental singlet triplet separations (Table VII) are determined from anticrossing measurements made at MIT and BTL. The values quoted here are for the $^3D_2$ level, not for the ^3D center of gravity as reported in I, II, and Table VI. The fine-structure constants of Table I were used to derive the results of Table VII from those of Table VI. The Grenoble values agree to within experimental error, and the $6d$ values measured at MIT and BTL agree. In addition, the $7d$ value agrees with the more accurate value of MacAdam and Wing.[28] The values from Martin's review,[18] based on optical spectra, lie within the error limits for the $3d$ and $4d$ levels, but are in error for the higher levels.

The calculation of Chang and Poe[8] does very well, although it predicts a separation about $\frac{1}{2}\%$ too small (Fig. 5). Chang[9] has pointed out that it should be possible to fit the separation with a function of the form

TABLE VII. Values (in GHz) of the $^1D_2$-$^3D_2$ separation in ^{4}He.

Level	This work	Other	Martin [a]	Theory [b] (Parish and Mires)	Theory [c] (Chang and Poe)	$a/n^3+b/n^5$ fit [d]
$3d$	102.36 ± 0.02 [e]		102.50	318.2	102.02	102.35
$4d$	59.14 ± 0.08 [e]		59.19	184.7	58.85	59.18
$5d$	34.125 ± 0.045 [e]		34.40	106.8	33.92	34.095
$6d$	20.946 ± 0.03 [f]		20.8	65.6	20.82	20.923
$7d$	13.646 ± 0.03 [g]	13.6568 ± 0.0002 [h]	14.8	42.8	13.56	13.629
$8d$	9.345 ± 0.035 [g,i]	9.337 ± 0.035 [j]	10.8	29.3	9.29	9.327

[a] Reference 18.
[b] Reference 29.
[c] Reference 8.
[d] $a = 5105 \pm 13$ GHz $= 170.3 \pm 0.4$ cm^{-1} and $b = -21070 \pm 300$ GHz $= -702.8 \pm 10$ cm^{-1}.
[e] Measurements made with Bitter magnet.
[f] Average of values derived from BTL and Bitter magnet measurements.
[g] Measurements made at BTL. See I and II.
[h] Reference 28.
[i] Corrected value. See footnote a to Table VI.
[j] H. J. Beyer and K. J. Kollath, J. Phys. B 8, L326 (1975), increased by 11 MHz to give the $^1D_2$-$^3D_2$ separation.

$$\Delta E = \frac{a}{n^3} + \frac{b}{n^5} + \frac{c}{n^7} . \tag{12}$$

The last column of Table VII shows the separation calculated from two terms where a and b were obtained by a least-squares fit to the experimental $3d$-$8d$ separations. The excellent agreement confirms the functional form. The values of a and b (footnote to Table VII) are nearly equal to those obtained by Chang,[9] $a = 169.63$ and $b = -708.20$ cm^{-1} (and $c = 26.33$ cm^{-1}) from a fit to the calculated singlet-triplet intervals of Chang and Poe.[8]

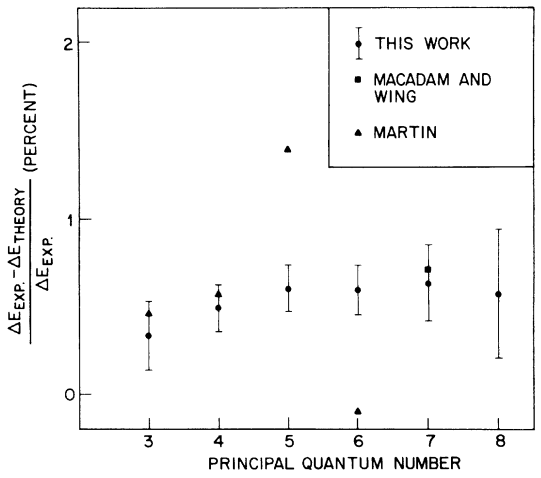

FIG. 5. Comparison between experiment and the theory of Chang and Poe (Ref. 8) for the $n\,^1D_2$-$n\,^3D_2$ separation. The optical measurements for $n = 7$ and $n = 8$ are off scale (respectively, at 8.4% and 14%).

B. Singlet-triplet mixing

A precise understanding of singlet-triplet mixing would be of considerable importance in spectroscopy. Helium, as the prototype system, is therefore the logical first step, and indeed a number of theoretical[29-35] and experimental[36-40] studies have been carried out. Several theoretical[29,30] and experimental[36] determinations have been made of singlet-triplet mixing in the D states of helium, but we shall see that all disagree with the present results, which, we believe, are the most reliable and accurate.

Let us define a singlet-triplet mixing coefficient ω. Let $\Psi(n^3D_J)$ and $\Psi(n^1D_J)$ be Russell-Saunders eigenfunctions of the Hamiltonian in the limit of infinitely large singlet-triplet separation. For finite values of the separation (and coupling) $\Psi(n^3D_1)$ and $\Psi(n^3D_3)$ remain eigenfunctions of the Hamiltonian. However, for $J = 2$, the eigenfunctions Φ are the orthonormal linear combinations

$$\Phi = a_s \Psi(n^1D_2) + a_t \Psi(n^3D_2) . \tag{13}$$

The mixing coefficient is defined as

$$\omega = a_s / a_t , \tag{14}$$

where a_s and a_t are appropriate for the Φ which, in the limit of infinite separation, becomes $\Psi(n^3D_2)$.

ω can be obtained exactly by diagonalizing the 2×2 matrix formed by the total Hamiltonian between the basis states $\Psi(n^1D_2)$ and $\Psi(n^3D_2)$. The diagonal elements are derived from the measured singlet-triplet separation (Table VII) and the off-diagonal elements from the measured off-diagonal

TABLE VIII. Values of the mixing parameter ω ($\times 10^3$) between the $^1D_2$ and the $^3D_2$ states at zero magnetic field.

Level	Parish and Mires [a]	Van den Eynde *et al.* [b]	MacAdam and Wing [c]	This work
$3d$	5.0	9.37		15.3 ± 0.7
$4d$	3.6	6.85		11.1 ± 0.8
$5d$	3.2	6.03		9.8 ± 0.7
$6d$	3.0	5.68		9.4 ± 0.5
$7d$	2.9	5.50	9.17	9.1 ± 0.7
$8d$	2.9	5.36		9.4 ± 1.0

[a] Reference 29.
[b] Reference 30.
[c] Reference 28.

spin-orbit parameter $\mathcal{A}$ (Table I).

It can be shown from Eq. (7) of I and angular momentum coupling relationships that the matrix element between $\Psi(n^1D_2)$ and $\Psi(n^3D_2)$ is $\sqrt{6}\,\mathcal{A}$. This is sufficiently smaller than the difference between the diagonal matrix elements that we can use first-order perturbation theory. Thus within experimental error

$$\omega \cong \sqrt{6}\,\mathcal{A}/\Delta E\,, \tag{15}$$

where ΔE can be taken, again within experimental error, as the experimental $^1D_2$-$^3D_2$ separation.

The values of ω obtained from Eq. (15) and Tables I and VII are given in Table VIII. The quoted error limits are based on the experimental errors given earlier for $\mathcal{A}$ and ΔE. As these are both direct experimental measurements and no further assumptions are made in the calculation of ω, we have every reason to believe in its absolute accuracy within these limits. The values of ω indicate about 1% singlet in the triplet wave function, decreasing slightly with n to a limiting value for large n, as first noticed by Van den Eynde *et al.*[30] The agreement with the $n = 7$ value of MacAdam and Wing[28] is excellent. That value is based on the off-diagonal spin-orbit matrix element calculated by the Breit theory[17] and the experimental ΔE.

The theoretical values of Parish and Mires[29] and Van den Eynde *et al.*[30] are in poor agreement with experiment, although the n dependence is similar. It is interesting that all of the Van den Eynde values are a factor of $\sim 1.6_3$ smaller than experiment and the Parish and Mires values are a factor of $\sim 3.0_8$ smaller. The error, as suggested by MacAdam and Wing,[28] may be in the neglect of second-order exchange terms. Chang and Poe[8] have shown that these second-order terms are quite large and of opposite sign to the first-order terms. The combined exchange energy[8] is 1.7 times smaller than the first-order term above; thus in an expression of the form of Eq. (15) such as Van den Eynde *et al.*[30] used, the mixing coefficient would become 1.7 times larger and essentially agree with experiment. Unfortunately, Van den Eynde *et al.* do not report intermediate steps in their calculation, so we cannot check this hypothesis.

In a similar way the results of Parish and Mires[29] are brought closer to experiment if multiplied by 1.7. However, even then, there exists substantial disagreement. Fortunately Parish and Mires did give intermediate results, including the values for ΔE given in Table VII. Comparing them with the present experimental results shows that the calculated ΔE values are all a factor of 3.1_3 too large. This factor nearly exactly accounts for the factor of 3.0_8 discrepancy found in their ω's.

Thus it appears that both theoretical calculations suffer in their treatment of the exchange separation. The off-diagonal coupling is apparently accurately calculated, as might be expected from the good agreement between the experimental values and those calculated from the simple hydrogenic theory listed in Table I.

To our knowledge there has been only one previous experimental determination of the mixing coefficient ω.[36] In that experiment He is excited by protons and the optical emission monitored. In the absence of singlet-triplet mixing, no light should be emitted from triplet states. Assuming small but finite mixing of singlet and triplet D states, ω^2 is given by the ratio of the optical emission from the ^1D and ^3D states so long as cascade effects from higher states can be neglected. A value of $\omega^2 = 0.06$ for the $n = 3$ $^{1,3}D$ state has been reported. This result[36] would imply that $\omega = 0.2$, while we see from Table VII that $\omega = 0.0153$. Thus one is forced to the conclusion that proton excitation does not give a good measure of ω, at least for D states. Indeed, the present results establish that more than 99% of

the light emitted from the ^3D state excited by proton impact must be due to cascade processes, e.g., from F states where singlet-triplet mixing is larger.[38]

Finally, we note that anticrossing experiments of the type presently described represent the first experimental means for determining directly the extent of singlet-triplet mixing in a state. The present results are precise to 5–10%, with no reason to suspect any systematic error. This accuracy suffices for present needs but does not in any way represent a limit to the precision obtainable by this technique. At the present ω is limited by uncertainties in $\mathcal{A}$, while $\mathcal{A}$ in turn is limited by inaccuracies in the line-shape deconvolution due to imprecise knowledge of excitation cross sections for different M states, noisy data, etc. Relatively simple experiments could be performed to reduce these uncertainties, and along with careful analysis could yield values of ω an order of magnitude more precise.

ERRATA

Errors in I and II are noted here. None influenced the results as much as the quoted experimental uncertainty and they have no effect on the conclusions, but for the benefit of future workers we mention them. The spin-spin term as given in II by the footnote to Table III should be divided by 2. A factor of $2L - 1$ in Eq. (19) of I should read $2L + 1$, as given by Eq. (7) of this work. The sign of the motional Stark effect should be reversed in I and II.

ACKNOWLEDGMENTS

We thank the Service National des Champs Intenses, part of the Centre National de la Recherche Scientifique, and the Max Plank Institute (Grenoble) which made possible the experiment at Grenoble, and we thank L. Rubin for his help and advice in carrying out the experiments at MIT.

---

*Work performed in part at the Service National des Champs Intenses of Grenoble (Centre National de la Recherche Scientifique), France.

†Laboratoire associe au Centre National de la Recherche Scientifique.

‡Part of this work performed while the authors were guest scientists at the Francis Bitter National Magnet Laboratory, which is supported at MIT by the National Science Foundation.

[1]T. A. Miller, R. S. Freund, F. Tsai, T. J. Cook, and B. R. Zegarski, Phys. Rev. A 9, 2474 (1974).

[2]T. A. Miller, R. S. Freund, and B. R. Zegarski, Phys. Rev. A 11, 753 (1975).

[3]R. Jost and M. Lombardi, Phys. Rev. Lett. 33, 53 (1974).

[4]T. A. Miller and R. S. Freund, J. Chem. Phys. 61, 2160 (1974).

[5]T. A. Miller, R. S. Freund, B. R. Zegarski, R. Jost, M. Lombardi, and J. Derouard, J. Chem. Phys. 63, 4042 (1975).

[6]R. T. Poe and T. N. Chang, At. Phys. 3, 151 (1973).

[7]T. N. Chang and R. T. Poe, Phys. Lett. 45A, 477 (1973).

[8]T. N. Chang and R. T. Poe, Phys. Rev. A 10, 1981 (1974); 14, 11 (1976).

[9]T. N. Chang, J. Phys. B 7, 408 (1974).

[10]M. Lombardi, J. Phys. Radium 30, 631 (1969); Ph.D. thesis (Grenoble, 1968) (unpublished).

[11]G. Adams (unpublished).

[12]N. Bessis, H. Lefevbre-Brion, and C. M. Moser, Phys. Rev. 135, A957, (1964).

[13]A. C. Tam, Phys. Rev. A 12, 539 (1975).

[14]D. Dily, Ph.D. thesis (Paris, 1970) (unpublished); D. Dily and J. P. Descoubes, C. R. Acad. Sci. B 272, 1182 (1971) (Note that Ref. 16 of Dily and Descoubes quotes an incorrect value for the $n=6$ $\Delta\nu_{12}$, which was used in II).

[15]J. P. Descoubes, *Physics of One and Two Electron Atoms* (North-Holland, Amsterdam, 1969), p. 341.

[16]H. G. Berry, J. L. Subtil, and M. Carre, J. Phys. Radium 33, 947 (1972), and references therein.

[17]H. A. Bethe and E. E. Salpeter, *Quantum Mechanics of One- and Two-Electron Atoms* (Springer, Berlin, 1957).

[18]W. C. Martin, J. Phys. Chem. Ref. Data 2, 257 (1973).

[19]W. L. Wiese, M. W. Smith, and B. M. Glennon, *Atomic Transition Probabilities* (Natl. Bur. Stand., U. S. GPO, Washington, 1966).

[20]A. H. Gabriel and D. W. O. Heddle, Proc. R. Soc. A 258, 124 (1960).

[21]E. U. Condon and G. H. Shortley, *The Theory of Atomic Spectra* (Cambridge U. P., Cambridge, England, 1967).

[22]U. Fano, Rev. Mod. Phys. 29, 74 (1957).

[23]A. Omont, J. Phys. Radium 26, 26 (1965); Ph.D. thesis (Paris, 1967) (unpublished).

[24]A. Omont and J. Meunier, Phys. Rev. 169, 92 (1968).

[25]J. P. Faroux, Ph.D. thesis (Paris, 1969) (unpublished).

[26]C. W. T. Chein, R. E. Barkeley, and F. W. Dalby, Can. J. Phys. 50, 116 (1972).

[27]M. Pinard and J. van der Linde, Can. J. Phys. 52, 1615 (1974); M. Pinard, Ph.D. thesis (Paris, 1973) (unpublished).

[28]K. B. MacAdam and W. H. Wing, Phys. Rev. A 12, 1464 (1975).

[29]R. M. Parish and R. W. Mires, Phys. Rev. A 4, 2145 (1971).

[30]R. K. Van den Eynde, G. Wieber, and Th. Niemeyer, Physica (Utr.) 59, 401 (1972).

[31]G. W. F. Drake, Phys. Rev. 181, 23 (1969).

[32]G. W. F. Drake and A. Dalgarno, Astrophys. J. 157, 459 (1969).

[33]B. Schiff, Y. Accad, and C. L. Pekeris, Phys. Rev. A 8, 2272 (1973), and references therein.

[34]A. F. J. van Raan and H. G. M. Heideman, J. Phys. B 7, L216 (1974).

[35]G. Araki, M. Okta, and K. Mano, Phys. Rev. 116, 651 (1959), and references therein.
[36]D. Krause and E. A. Soltysik, Phys. Rev. A 6, 694 (1972).
[37]R. B. Kay and R. H. Hughes, Phys. Rev. 154, 61 (1967); R. B. Kay and J. G. Showalter, Phys. Rev. A 3, 1998 (1971), and references therein.
[38]R. M. St. John and R. G. Fowler, Phys. Rev. 122, 1813 (1961), and references therein.
[39]C. C. Lin and R. M. St. John, Phys. Rev. 128, 1749 (1962).
[40]R. M. St. John and T. W. Nee, J. Opt. Soc. Am. 55, 426 (1965).